DEVELOPMENT AND EVALUATION OF CARBON-BASED MERCURY ADSORBENTS

Massoud Rostam-Abadi[1,2], Hsing-Cheng Hsi[2], Christopher M. B. Lehmann[2], Mark J. Rood[2], and Ramsey Chang[3]

[1] Illinois State Geological Survey, Champaign, IL 61821

[2] Department of Civil and Environmental Engineering, University of Illinois at Urbana-Champaign, Urbana, IL, 61801,

[3] EPRI, Palo Alto, CA, 94304

Introduction

Activated carbon injection upstream of a particulate control system is currently the most viable method available for removal of both elemental and oxidized mercury from coal-fired utility flue gas streams [1]. However, current estimates predict very high costs associated with mercury control, with activated carbon costs representing a large fraction of the overall costs. In order to make carbon injection for mercury removal feasible, it is necessary to either reduce the amount of carbon needed, or decrease the cost of activated carbon production.

The cost of activated carbon production is determined by the availability and cost of precursor materials and the required processing steps for activation. The use of inexpensive precursors along with simple activation steps should lower the production costs. However, activated carbons produced from different precursor materials will have differing properties and adsorption performances, due to inherent variations in the chemical and physical nature of precursor materials.

In this work, activated carbons were prepared from a variety of precursor materials including a high-sulfur coal, pistachio nut shells, and waste tire rubber. In addition to these adsorbents, a lignite-based commercial activated carbon and phenolic polymer activated carbon fibers were evaluated in laboratory tests to determine their abilities to remove both elemental mercury and mercuric chloride in simulated coal combustion flue gases.

Experimental

Pistachio shell-, and tire-derived activated carbons were prepared in a pilot-scale rotary kiln. A high-organic-sulfur Illinois bituminous coal-derived activated carbon was prepared in a pilot-scale fluidized-bed reactor. Carbonization and activation were used to prepare all samples. The commercial activated carbon and the activated carbon fibers tested were Darco FGD (American Norit Inc.) and ACF-5092-20 (American Kynol Inc., Pleasantville, NY).

The precursors were analyzed for their moisture, ash, carbon, hydrogen, nitrogen, and total sulfur contents using standard ASTM methodology (Table 1). The surface area and pore structure properties of carbon adsorbents were evaluated via nitrogen adsorption (at 77 K). Nitrogen adsorption isotherms were determined via an adsorption apparatus (Micromeritics ASAP 2400). Surface areas were determined via the standard BET equation. Total pore volumes were determined at $P/P_0 \approx 0.98$. Micropore surface areas, volumes, and distributions were evaluated using the 3-D pore size distribution model developed at ISGS-UIUC [2].

Elemental mercury (Hg^0) and mercuric chloride ($HgCl_2$) equilibrium adsorption capacities for prepared samples were completed by URS Radian (Austin, TX). Mercury adsorption tests were carried out with a fixed-bed reactor using different simulated coal-combustion flue gas conditions with a mercury (Hg^0 or $HgCl_2$) concentration of 50±20 μg/Nm^3 at 163 °C (Table 2), with the balance comprised of representative concentrations of O_2, CO_2, H_2O, and N_2. To simulate combustion flue gases from Eastern bituminous (EBC), low-sulfur Eastern bituminous (LSEBC) and Western sub-bituminous (WSC) coal combustion, various concentrations of HCl, SO_2 and NO_x were added to the gas streams. A detailed description of mercury adsorption tests is given elsewhere [3].

Results and Discussion

Proximate analyses of the Illinois coal, tire, and pistachio shells indicate that the principle differences in these precursor materials are in the ash, sulfur, and carbon contents (Table 1). The ash content of pistachio shells is negligible in comparison with the coal and tire. Total sulfur contents of the precursors also differed, again with pistachio having a negligible sulfur content in comparison to the coal and tire precursors. Sulfur contents are of interest, since they likely influence the adsorption of mercury species.

Properties of activated carbons and activated carbon fibers are presented in Table 3. For the prepared activated carbons, the pistachio carbon had the lowest ash and sulfur contents followed by the coal and tire carbons. The surface area of the tire carbon

(280 m^2/g) was about one-half of the coal and pistachio carbons. Tire carbon, however, had between 13 and 40% larger total pore volume (0.433 vs 0.301 and 0.315 cc/g) in comparison with the coal and pistachio carbons. Pistachio carbon was more microporous than coal and tire carbons; about 94% of the pores in the pistachio carbon were in the micropore range as compared to about 80% for the coal and tire carbons. Tire-derived activated carbons with surface areas as large as 1000 m^2/g, and micropore volumes as large as 0.5 cc/g were prepared in bench-scale facilities in this study. The reactivity and pore structure data for these carbons suggest that there should not be any difficulties in developing porosity in tire-derived char.

During the pilot-scale production of the pistachio carbon, several samples of carbonized pistachio shells were collected. These samples were not activated and are designated as pistachio shell char (PSC). PSC had low sulfur and ash contents and was highly microporous; micropore area contributed about 93% of the total surface area (386 m^2/g).

FGD carbon had the largest ash content (32.1 wt%) and the smallest micropore area to total surface area ratio (0.45) among the activated carbons tested. FGD has been extensively studied for removal of mercury emissions from flue gases generated from coal, municipal, and hazardous waste combustion flue gases [3].

ACF-20 had no sulfur and ash content. The surface area of this carbon was 1971 m^2/g with micropores contributing 95% of the total surface area. Micropore volume of ACF-20 (0.949 cc/g) was more than 100% larger than the coal, tire, and pistachio carbons and 50% lager than FGD carbon. Micropore size distributions (Figure 1) of the ACF-20, coal, PSC, FGD revealed that these carbons had comparable distributions of pores in the micropore region, dominated by pores in the range of 5 to 10 Å. Although not presented, tire and pistachio carbon had comparable micropore size distributions. Mesopore size distributions of the carbons were also measured, but are not presented in this paper. Because the concentrations of mercury species are very small in the coal-fired utility flue gases (1 to 10 $\mu g/Nm^3$), the more energetic micropores are expected to be more efficient than meso- or macro-pores in capturing mercury.

With a few exceptions, mercury adsorption data at different gas compositions generally showed that the activated carbons had comparable adsorption capacities (Table 4). However, some difference were observed with individual carbon samples at different gas compositions tested. Lowering the concentration of acid gas components (SO_2 and HCl) resulted in higher $HgCl_2$ adsorption capacities. For the coal-derived carbons, including FGD, higher Hg^0 adsorption capacities were also observed as the acid components in the gas were lowered. Tire carbon, however, performed better in the EBC flue gas which had the largest SO_2 concentration. Pistachio carbon generally performed better than other carbons in capturing Hg^0, although there was not a general trend from one gas composition to another. The Hg^0 adsorption capacities of the PSC and the ACF-20 were comparable and smaller than the other carbons tested. Mercury adsorption results indicate that each sample may be affected by gas composition in a unique way. For each carbon, however, the adsorption of $HgCl_2$ appeared to be less affected by changes in gas composition than observed for Hg^0.

Neither the physical properties, such as total surface area and micropore area, nor the total sulfur in the samples alone appeared to impact mercury adsorption capacity. It is interesting to note that although the micropore area of the highly microporous ACF-20 was about 3 to 8 times larger than the other activated carbons. This sample's Hg^0 adsorption capacity was smaller than all of the tested carbons (except for tire carbon under LSEBC gas composition). These results indicate that highly microporous carbons without any active surface functional groups, such as sulfur, do not have large capacity for mercury adsorption. For example, by increasing the micropore area of the PSC from 386 to 559 m^2/g while retaining the sulfur (0.06 wt%) in the pistachio carbon (see data in Table 2), the Hg^0 capacity increased two to three fold. This sample's mercury adsorption capacities were comparable to, and in some gas compositions larger than, the coal and tire carbons which had higher total sulfur contents.

With the limited data presented in this paper, it is difficult to draw any conclusions on the roles of microporosity and active sulfur functional groups on mercury adsorption. These data, however, indicate that both microprosity and sulfur functional groups are potentially important parameters in enhancing Hg^0 adsorption capacity of a carbon-based adsorbent. It is well known that sulfur impregnation enhances mercury adsorption capacity of activated carbon [4]. However, the nature and the role of the sulfur active sites in capturing mercury in coal combustion flue gas have not been established. Future research in this area should help design and manufacture activated carbons with enhanced capacities for mercury adsorption.

This research has shown that relatively inexpensive agricultural byproducts, such as pistachio shell and potentially other biomass materials, and waste tire rubber are desirable precursors for producing low-cost mercury adsorbents.

References

1.Chang R., Owens D., Developing mercury removal methods for power plants, *EPRI Journal* **1994**, July/August: 46-49.

2. Sun J., Chen S., Rood M.J., Rostam-Abadi M., Correlating N2 and CH4 adsorption on microporous carbon using a new analytical model, *Energy and Fuels* **1998**, 12 (6): 1071-1078.

3. Carey T.R., Hargrove O.W. Jr., Richardson C.F., Chang R., Meserole, F.B., Factors affecting mercury control in utility flue gas using activated carbon, *Journal of Air & Waste Management Association* **1998** 48: 1166-1174.

4. Hsi H.C., Rostam-Abadi M., Rood M.J., Chen S., and Chang R, "Preparation of Sulfur-Impregnated Activated Carbon Fiber Clothes (ACFCs) for Removal of Mercury Vapor from Simulated Combustion Flue Gases," in *Proceedings: **93rd Annual Air & Waste Management Association***, Salt Lake City, Utah, June 2000, Abstract no. 435, p. 12

Table 1. Properties of raw sorbent materials

	coal	raw tire	pistachio shell
Moisture	9.3	0.5	4.4
Ash[a]	11.5	3.0	0.2
Carbon[a]	68.1	87.2	48.0
Hydrogen[a]	4.8	7.6	6.1
Nitrogen[a]	1.2	0.2	0.1
Oxygen[a b]	10.5	0.9	45.5
Total sulfur[a]	3.7	1.6	0.2

[a] moisture-free values; [b] oxygen content determined by difference

Table 2. Simulated coal-combustion flue gas composition in mercury adsorption tests

Condition*	SO_2	HCl (ppmv)	NO_x	O_2	CO_2 (v/v %)	H_2O
Eastern bituminous coal (EBC)	1600	50	400	6	12	7
Low-sulfur eastern bituminous coal (LSEBC)	400	50	400	6	12	7
Western subbituminous coal (WSC)	400	2	200	6	12	7

Table 3. Properties of adsorbents

	coal	tire	pistachio shell	PSC	FGD	ACF-20
Ash [wt. %]	18.7	25.1	9.8	6.1	32.1	0.0
Sulfur content	1.2	2.1	0.06	0.07	0.98	0.0
Surface area [m^2/g]	695	280	559	386	503	1971
Micropore area [m^2 /g]	563	220	524	361	228	1886
Total pore volume [cc/g]	0.391	0.443	0.315	0.208	0.636	0.949

Table 4. The equilibrium Hg^0 and $HgCl_2$ adsorption capacities (mg/g) of carbon adsorbents at 163 °C and 50 µg/m^3 inlet mercury concentration.

Sample Code	Equilibrium Hg^0 Adsorption Capacity			Equilibrium $HgCl_2$ Adsorption Capacity		
Flue gas condition	EBC	LSEBC	WSC	EBC	LSEBC	WSC
Coal	421	579	857	425	505	542
Tire	803	218	402	709	146	751
Pistachio	687	1129	762	522	256	503
PSC	341	347	-	174	-	-
FGD	638	575	1065	646	854	848
ACF-20	359	319	-	-	-	-

[a] EBC: eastern bituminous coal; LSEBC: low-sulfur eastern bituminous coal; WSC: western subbituminous coal.

[b] - = not available

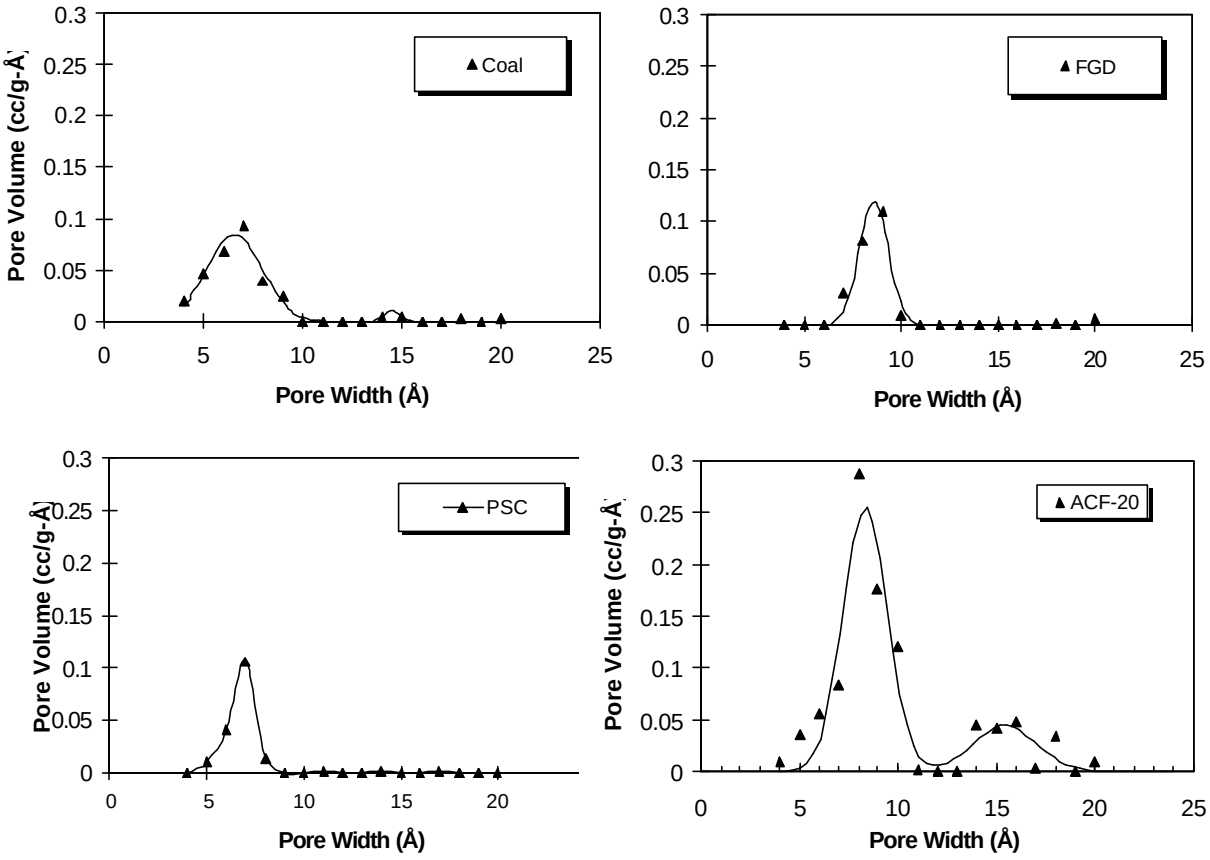

Figure 1. Pore Size Distribution of coal, FGD, PSC and ACF-20